

3,3'-Diindolylmethane (DIM) is a novel topoisomerase II α catalytic inhibitor that induces S phase retardation and mitotic delay in human hepatoma HepG2 cells

Yixuan Gong, Gary L. Firestone and Leonard F. Bjeldanes

Department of Nutritional Sciences and Toxicology, University of California, Berkeley, CA 94720-3104: YG, LFB

Department of Molecular and Cell Biology, University of California, Berkeley, CA 94720-3104: GLF

Running title: DIM inhibits topo II α and cell cycle progression

Send correspondence to:

Leonard F. Bjeldanes
Department of Nutritional Sciences and Toxicology
119 Morgan Hall
University of California
Berkeley, CA 94720-3104
Phone: (510)642-1601, Fax: (510)642-0535
Email: lfb@nature.berkeley.edu

Abbreviations:

3,3'-diindolylmethane, DIM; 4',6-diamidino-2-phenylindole, DAPI; 7,12-dimethylbenz(a)anthracene, DMBA; concentration of half maximal inhibition, IC₅₀.

The number of text pages: 25

The number of tables: 0

The number of figures: 10

The number of references: 39

The number of words in the Abstract: 182

The number of words in the Introduction: 615

The number of words in the Discussion: 951

ABSTRACT

Epidemiological evidence suggested that high consumption of *Brassica* genus vegetables, such as broccoli, cabbage and Brussels sprouts, is very effective in reducing the risks of several types of cancers. 3,3'-Diindolylmethane (DIM), one of the most abundant and biologically active dietary compounds derived from *Brassica* vegetables, displays remarkable antitumor activity against several experimental tumors. In the present study, we demonstrate for the first time that DIM is a novel catalytic topoisomerase II α inhibitor. In supercoiled DNA relaxation assay and kinetoplast DNA decatenation assay, DIM strongly inhibited DNA topoisomerase II α and also partially inhibited DNA topoisomerase I and II β . DIM did not stabilize DNA cleavage complex, nor did it prevent etoposide-induced DNA cleavage complex formation. Further experiments showed that DIM inhibited topoisomerase II α -catalyzed ATP hydrolysis, which is a necessary step for the enzyme turnover. In cultured human hepatoma HepG2 cells, DIM blocked DNA synthesis and mitosis in a concentration-dependent manner, which was consistent with the outcome of topoisomerase inhibition in these cell cycle phases. Our results identified a new mode of action for this intriguing dietary component that might be exploited for the therapeutic development.

INTRODUCTION

Certain indole derivatives from *Brassica* vegetables are under study for their potential cancer protective activities (Chang et al., 2005; Dashwood et al., 1994; Firestone and Bjeldanes, 2003). Indole-3-carbinol (I3C), found in the *Brassica* vegetables such as broccoli, cabbage and Brussels sprouts, inhibited tumor development in mammary gland, liver, uterus, stomach and other organs, when administered orally to rodents before or during carcinogen exposure (Dashwood et al., 1994; He et al., 1997; Oganessian et al., 1997; Takahashi et al., 1995). 3,3'-Diindolylmethane (DIM) is one of the major products of I3C that are formed in gastric acid (De Kruif et al., 1991; Leibelt et al., 2003; Staub et al., 2002). DIM induces the expression of phase 1 and phase 2 xenobiotic metabolizing enzymes in the liver and extrahepatic tissues, resulting in the enhanced capacity for detoxification of carcinogens (Chen et al., 1996; Gross-Steinmeyer et al., 2004; Lake et al., 1998; Renwick et al., 1999; Sanderson et al., 2001). Studies clearly showed that DIM administered orally at the dose of 5 mg/kg body weight for 21 days effectively inhibited mammary gland tumor growth by 80% in female Sprague-Dawley rats that were initiated with mammary gland carcinogen 7,12-dimethylbenz(a)anthracene (DMBA) (Chen et al., 1998). Results of studies conducted in our laboratory further demonstrated that DIM significantly inhibited the growth of human breast tumor xenografts (MCF-7) in athymic mice (Chang et al., 2005). Since the growth of xenograft tumors does not rely on carcinogen exposure, detoxification of carcinogen does not explain the growth inhibitory effects of DIM on xenograft tumors. Thus, other mechanisms must be considered.

DNA topoisomerases (topos) are nuclear enzymes that regulate conformational changes in DNA topology by catalyzing the breakage and resealing of DNA strands. In humans, there are 6 topoisomerase genes encoding for nuclear topoisomerase I (topo I), mitochondrial topo I, topo II α and β and topo III α and β (Champoux, 2001; Wang, 2002). Although the functions of some of these enzymes

are still not clear, they are extremely important in relaxing supercoiled DNA generated during major cellular processes such as DNA replication, RNA transcription and DNA recombination. In addition, topo II is indispensable during mitosis in separating the extensively intertwined sister chromatids due to its decatenation activity (Chang et al., 2003; Clarke et al., 1993). Topoisomerase inhibitors are one of the most widely studied and clinically used classes of anticancer agents (Denny and Baguley, 2003; Larsen et al., 2003; Pommier et al., 1998; Wang, 2002). Topoisomerase inhibitors can be divided into two classes according to their mechanisms of action (Larsen et al., 2003; Topcu, 2001). The class I drugs including camptothecin, etoposide, anthracyclines, ellipticines, epipodophyllotoxins, and etc, are also called topoisomerase poisons, because they are able to stabilize a reversible, covalent DNA-topoisomerase complex (called the DNA cleavage complex), which is a normal reaction intermediate in the catalytic cycle of the enzymes. Class II topoisomerase inhibitors, which include a variety of structurally diverse compounds, interfere with different steps in the catalytic cycle of the enzymes without trapping the covalent complex (Larsen et al., 2003). The drugs in this class are referred to as topoisomerase catalytic inhibitors, such as aclarubicin, merbarone, and bisdioxopiperazines.

In the present study, we demonstrate for the first time that DIM strongly inhibited DNA topo II α and partially inhibited DNA topo I and II β , without stabilizing DNA cleavage complex. To illustrate the mechanism of DIM-induced topo II α inhibition, we found that DIM did not inhibit the steps prior to DNA cleavage in the enzyme catalytic cycle; instead, it inhibited topo II α -catalyzed ATP hydrolysis, which is a necessary step for enzyme turnover. The topoisomerase inhibition was further confirmed in cultured HepG2 cells by demonstrating that DIM inhibited S phase progression and chromosome segregation.

MATERIALS AND METHODS

2.1 Chemicals

Salmon sperm DNA and all the cell culture reagents except fetal bovine serum (Omega Scientific Inc, Tarzana, CA) were from GIBCO/Invitrogen (Carlsbad, CA). DIM was purchased from LKT Laboratory Inc (St. Paul, MN). RNase, propidium iodide (PI), aclarubicin, amsacrine (m-AMSA), thymidine, 4',6-Diamidino-2-phenylindole (DAPI) and nocodazole, were from Sigma (St. Louis, MO). ^3H -deoxythymidine (^3H -dT) and γ - ^{32}P -ATP (3000 Ci/mmol stock) were purchased from Perkin-Elmer (Boston, MA). Topo I, topo II α , topo I/II drug screening kits and topo II assay kit were purchased from Topogen Inc (Columbus, Ohio). Topo II β was purchased from LAE Biotech International (Rockville, MD). Comet assay kit was from Trevigen Inc. (Gaithersburg, MD). All other reagents were of the highest grade available.

2.2 Cell culture and cell growth curve determination

The human hepatoma cell line HepG2 was obtained ATCC and were cultured in 10-cm petri dishes in DMEM supplemented with 10% fetal bovine serum, 100 U/ml penicillin and 100 U/ml streptomycin in a humidified incubator with 5% CO_2 at 37 °C. To determine the cytostatic effects of DIM, HepG2 cells were seeded at a density of $5 \times 10^4/\text{ml}$, and after 24 hours, were treated with different concentrations of DIM. The number of DIM-treated cells was counted for three successive days using Coulter® particle counter (Beckman Coulter, Fullerton, CA).

2.3 DIM-DNA interaction

The absorption spectra of DIM were determined on a Beckman DU®530 spectrometer. Using the maximal absorbance at 280 nm as the excitation wavelength, the fluorescence emission spectra of DIM

were recorded on a Perkin-Elmer 650 10S fluorescence spectrometer in a range of 300 nm to 460 nm, using a slit width of 5 nm. After obtaining the maximal emission wavelength, a fluorescence titration experiment was performed by keeping the DIM concentration constant at 30 μ M in PBS solution, stoichiometrically varying the sheared salmon sperm DNA concentration and recording the DIM fluorescence. In addition, an ethidium bromide displacement experiment was employed to determine whether DIM intercalated into DNA. Fluorescence spectra (excitation wavelength at 610 nm and emission wavelength at 475 nm) were obtained at 25 °C on a Perkin-Elmer 650 10S fluorescence spectrometer. The assay buffer contained 0.5 μ g/ml ethidium bromide, 5 μ g/ml sheared salmon sperm DNA and 0-75 μ M DIM or m-AMSA in PBS solution. The fluorescence of 0 μ M DIM was set as 100%.

2.4 Topoisomerase relaxation assay and cleavage complex formation assay

Topo I, topo II α and topo II β -mediated supercoiled DNA relaxation assays and cleavage complex formation assays were performed using Topogen topoisomerase I and II drug screening kits according to the manufacturer's instruction. Topo II α and topo II β -mediated KDNA decatenation assays were performed using Topogen topoisomerase II assay kit as instructed by the manufacturer.

2.5 Determination of ATP hydrolysis

ATPase assay was performed as previously described by Osheroff et al. with modifications (Osheroff, 1986; Osheroff et al., 1983). The reaction buffer contained the indicated amounts of topo II α , 10 μ g sheared salmon sperm DNA, 1 mM γ -³²P-ATP (3000 Ci/mmol stock, Perkin-Elmer), and different concentrations of DIM (in 1% final DMSO v/v) in a total volume of 20 μ L. Reactions were started by the addition of topo II α and incubated at 37°C for 15 min. The reactions were stopped by 10 μ L of stopping buffer containing 4 M formic acid, 2 M LiCl and 36 mM ATP. Samples (3 μ L) were spotted

onto polyethylenimine-cellulose thin layer chromatography sheets (Analtech, Newark, DE). The sheets were developed in freshly-made 1 M formic and 0.5 M LiCl solution and analyzed by autoradiography. The areas corresponding to the free inorganic phosphate were cut out and quantified by scintillation counting.

2.6 Single cell electrophoresis assay/comet assay

HepG2 cells were seeded at a density of 5×10^5 /ml into 6-well plates and treated as described. After the indicated incubation times, cells were collected by gentle trypsinization and re-suspended in cold PBS. The following steps were carried out using Trevigen CometAssay™ kit. Briefly, cells were mixed with low melting point agarose, lysed at 4 °C for 60 min, denatured in alkaline solution for 30 min and then electrophoresed in TBE buffer at 1 volt/cm for 10 min. After air-drying, the slides were stained with SYBR® Green DNA fluorescent dye (494 nm / 521 nm) and observed. Digital images were captured on a Zeiss Axiophot microscope equipped with Qimaging camera.

2.7 Cell synchronization and flow cytometry

Cells were synchronized at G1-S boundary by a double thymidine block. Briefly, exponentially growing HepG2 cells were sequentially treated with 2 mM thymidine for 16 hours, fresh complete medium for 10 hours, and 2 mM thymidine for another 16 hours. Metaphase cells were synchronized by treating HepG2 cells with 0.04 µg/ml nocodazole for 24 hours. The mitotic cells were collected by gentle shaking.

To perform flow cytometry cell cycle analysis, HepG2 cells were seeded at a density of 5×10^5 /ml into 6-well plates and treated as described. After indicated incubation times, cells were collected and resuspended in PBS containing 200 µg/ml RNase, 50 µg/ml PI, 0.1% sodium citrate and 0.1% (v/v)

TritonX-100. Flow cytometry was performed on a Beckman-Coulter EPICS XL flow cytometer and data were processed by WinMDI 2.8 software.

2.8 Thymidine incorporation assay

Cells were seeded at a density of 2×10^5 /ml into 24-well plates and treated as described. At the end of the treatment, 3 μ Ci of ^3H -dT was added into the medium and allowed to incubate for 1 hour. After three gentle washes with cold 10% TCA, 500 μ L of 0.3 N NaOH was added. The lysate was transferred into opaque scintillation vials after 1 hour incubation. The amount of ^3H -dT incorporated into DNA was counted in a scintillation counter.

2.9 Confocal microscopy

HepG2 cells were seeded into coverslip-containing 6-well plates and treated as described. After rinsing with PBS, slides with attached cells were immersed in 4% paraformaldehyde solution for 10 min at room temperature followed by 10 min permeabilization with 0.2% Triton X-100 solution. Slides were mounted in antifading solution with DAPI (2 μ g/ml) and the digital images were obtained with a Zeiss LSM510 Meta confocal microscope.

2.10 Statistic analysis

The statistical differences between groups were determined using student t-test. Statistical significance are noted at the level of $p < 0.05$. The results are expressed as means \pm standard deviation(S.D.) for at least three replicates for each assay.

RESULTS

3.1 DIM exerts cytostatic effect in HepG2 cells

To determine the effects of DIM on cell proliferation, human hepatoma HepG2 cells were treated with 0-75 μ M DIM for up to 72 hours. The results shown in Fig. 1A indicated that DIM exhibited concentration-dependent growth inhibitory effects in HepG2 cells. DAPI staining showed that the nuclei of 75 μ M DIM-treated cells were shrunken and irregular, in comparison to the normal round-shaped nuclei seen in control cells (Fig. 1B).

3.2 DIM interacts with DNA *in vitro*

Previous studies in our laboratory showed that DIM was rapidly taken into the cells and was highly concentrated in the nuclear fraction (unpublished data). Therefore, it was of interest to determine whether DIM could interact with DNA. Fluorescence titration assay was carried out to determine DIM-DNA interaction. With an excitation wavelength of 280 nm, we observed that DIM gave maximal fluorescence at the wavelength of 370 nm in a concentration-dependent manner (Fig. 2A). Addition of increasing concentrations of sheared salmon sperm DNA gradually decreased fluorescence intensity of DIM by 30% (Fig. 2B). The emission wavelength exhibited a blue shift of ~5-10 nm upon increasing DNA concentration. From the above fluorescent titration experiment, we concluded that DIM could interact with DNA *in vitro*.

To further examine whether DIM intercalated into DNA, we performed an ethidium bromide displacement experiment, in which the binding of another DNA intercalator will competitively displace ethidium bromide from DNA, thus decreasing the ethidium bromide fluorescence. As shown in Fig. 2C, increasing concentrations of m-AMSA, a well-known DNA intercalator, gradually displaced ethidium bromide, as indicated by a strong concentration-dependent reduction in ethidium bromide fluorescence.

However, addition of DIM had a small effect on ethidium fluorescence (up to a maximum of 20% reduction). This result indicated that DIM is only a weak DNA intercalator.

3.3 DIM inhibits topoisomerases

DNA topoisomerases are among the most sensitive targets of DNA-interacting molecules. In our study, the effects of DIM on human topo I, II α and II β were investigated using supercoiled DNA relaxation assay and kinetoplast DNA (KDNA) decatenation assay. Results presented in Fig. 3A showed that camptothecin, positive control, strongly inhibited topo I-mediated supercoiled pBR322 relaxation. DIM showed some inhibitory effect on topo I, but the inhibition was not complete even at the highest DIM concentrations examined. In contrast, DIM exhibited much stronger inhibitory effect on topo II α , as shown in Fig. 3B and C. At concentrations above 10 μ M, DIM concentration-dependently inhibited topo II α -catalyzed supercoiled pRYG relaxation and KDNA decatenation, as did positive control etoposide. The inhibition reached almost 100% at DIM 25 μ M. However, in topo II β -mediated KDNA decatenation assay (shown in Fig. 3D), DIM showed no obvious effect until the concentration reached 75 μ M, indicating that topo II β was less sensitive to DIM than II α .

3.4 DIM blocks cell cycle progression in HepG2 cells

Next we determined whether the inhibition of topoisomerases by DIM would lead to cell cycle perturbation. For the experiment, HepG2 cells were synchronized at the G1-S boundary by double thymidine block. Two hours after the block was released, cells were treated with different concentrations of DIM and collected at the indicated times for flow cytometry DNA content analysis. The results presented in Fig. 4 showed that DIM concentration-dependently blocked cell cycle progression. Most of control cells progressed into G2/M phase nine hours after the release; DIM-treated cells, however, were

concentration-dependently retarded in S phase. DIM 100 μ M almost completely abolished the S phase progression. Twelve hours after the release, when control cells had finished mitosis and progressed back into G1, DIM 50 μ M-treated cells were delayed in G2/M phase, and DIM 75 and 100 μ M-treated cells were still in S phase. The response of synchronized cells to DIM clearly showed that DIM inhibited S phase progression and mitosis.

3.5 DIM inhibits DNA synthesis in cultured cells

In a further experiment, we performed a 3 H-dT incorporation assay to quantitatively measure the negative impact of DIM on DNA synthesis. The results presented in Fig. 5 show that during the first hour of exposure, DIM rapidly and strongly inhibited DNA synthesis in a concentration-dependent manner (IC_{50} of ~ 30 μ M). We conducted a further experiment to determine whether the inhibition was reversible. One hour after DIM exposure, cells were gently washed with PBS and reincubated in DIM-free medium. Considering that it takes time for DIM to be completely removed from cells due to its lipophilic nature, the rates of DNA synthesis were measured 1 hour and 4 hours after recovery. The results showed that DNA synthesis was gradually and significantly restored in all DIM-treated groups. For DIM 100 μ M-treated cells, 3 H-dT incorporation rate increased from 4% to 75% of control after 4 hours of recovery. Taken together, the results indicate that DIM was very effective in inhibiting DNA synthesis and that the effect of short term DIM treatment was reversible.

3.6 DIM interferes with mitosis

It is well established that topo II α s, especially topo II α , are critical for successful mitotic chromosome condensation and segregation (Chang et al., 2003; Clarke et al., 1993; Cortes et al., 2003). Since DIM strongly inhibited topo II α *in vitro*, we next asked whether DIM affected mitotic

chromosome segregation. For the experiment, we synchronized HepG2 cells in early mitosis by nocodazole treatment. Immediately after release, cells were treated with different concentrations of DIM or 10 μ M aclarubicin, a known topo II inhibitor (Sorensen et al., 1992). Four hours later, the remaining mitotic cells were counted after DAPI staining. The results in Fig. 6 show that more than 90% of the control cells finished mitosis in four hours, but DIM-treated cells were concentration-dependently retarded in mitosis. They were arrested in the different stages of mitosis and in some extreme cases, the chromosomes appeared abnormal, such as with entangled sister chromatids during anaphase (in Fig. 7). Therefore, DIM indeed adversely affected the separation of sister chromatids, which is consistent with the outcome of topo II α inhibition.

3.7 DIM does not stabilize DNA-cleavage complex *in vitro* or in cells

Topoisomerase poisons such as camptothecin and etoposide interfere with the religation step of topoisomerases by stabilizing the DNA-cleavage complex (Champoux, 2001; Osheroff, 1986; Pommier et al., 1998). To investigate whether DIM is a topoisomerase poison, a cleavage complex assay was performed (Fig. 8 A and B). The positive control camptothecin stabilized topo I cleavage complex as expected, resulting in the formation of open circular DNA that migrated more slowly during electrophoresis than did supercoiled DNA. However, no open circular DNA was formed following incubation with different concentrations of DIM. Similar results were obtained in the experiments with topo II α . The positive control etoposide stimulated formation of cleavage complex after incubation with topo II α , as indicated by the appearance of both open circular and linear DNA, neither of which was seen in DIM-containing reaction mixtures. These results indicated that DIM did not stabilize DNA-cleavage complex *in vitro*.

This conclusion was further justified by the results of single cell electrophoresis assay (comet

assay). It is known that DNA-cleavage complexes produced by topoisomerase poisons are converted into DNA strand breaks in cells through collision with DNA replication or RNA transcription machinery (Pommier et al., 1998). To evaluate whether DIM generated DNA damage in cultured cells, single cell gel electrophoresis assay was employed. The results presented in Fig. 8 C-E show that only 1 hour of 10 μ M etoposide treatment caused obvious comet-shaped nuclear staining, which is characteristic of extensive DNA damage in cells. However, up to 6 hours of DIM 75 μ M treatment caused no DNA damage, although this concentration was high enough to severely interfere with DNA synthesis and mitosis. Taken together, these results showed that DIM strongly inhibited II α , but it did not stabilize the cleavage complex in cells, nor did it cause DNA damage. Thus, DIM may be classified as topo II α catalytic inhibitor.

3.8 DIM has no effect on etoposide-induced DNA cleavage complex formation

Since we showed previously that DIM interacted with DNA in the fluorescence titration assay, we conducted a gel shift assay to examine whether DIM could interfere with the binding of topo II α to DNA. The results showed that aclarubicin, the positive control, completely blocked the binding of topo II α to the DNA probe. However, DIM (up to 200 μ M) did not affect enzyme-DNA binding (results not shown).

Previous studies have shown that if a catalytic inhibitor blocks topo II at the step prior to DNA cleavage, it will antagonize topoisomerase poison-induced cleavage complex formation (Fortune and Osheroff, 1998; Sorensen et al., 1992). The simplest explanation for the observation is that the catalytic inhibitor locks the enzyme in a prior step, thus reducing the level of catalytically active enzyme available for the action of topoisomerase poison. We co-administered DIM and etoposide in the DNA cleavage assay to determine whether DIM could block etoposide-induced DNA cleavage. The results

indicated that unlike positive control aclarubicin, DIM (up to 100 μ M) had no effect on etoposide-induced DNA cleavage (Fig. 9). These results indicate that DIM does not block the steps prior to DNA cleavage.

3.9 DIM inhibits topo II α ATPase activity

One remaining step to be examined in the topo II α catalytic cycle is ATP hydrolysis. Antitumor drugs such as bisdioxopiperazines inhibit topo II by inhibiting ATP hydrolysis thus trapping the enzyme in the form of a closed protein clamp (Berger et al., 1996; Osheroff, 1986; Roca et al., 1994). We monitored the effect of DIM on topo II α -catalyzed ATP hydrolysis by thin layer chromatography (Fig. 10). The result showed that DIM concentration-dependently inhibited the ATP hydrolysis. When 200 units of enzyme were used, ~40% inhibition was observed, but when only 20 units of enzyme were used, the inhibition of ATP hydrolysis reached up to ~77%. Therefore, DIM inhibited human topo II α -mediated ATP hydrolysis, a key step necessary for enzyme turnover.

DISCUSSION

In this study, we provide evidence for the first time that DIM is a human topo II α inhibitor. Our results showed that DIM could completely block topo II α -catalyzed supercoiled DNA relaxation and KDNA decatenation, and partially inhibit topo I-mediated supercoiled DNA relaxation. The effect of topoisomerase inhibition was also characterized in cultured HepG2 cells by demonstrating that DIM arrested G1-S synchronized HepG2 cells at S phase and G2/M phase. In a further 3 H-dT incorporation assay, we showed that DIM inhibited DNA synthesis in a clear concentration-dependent manner and the inhibition occurred rapidly after DIM exposure and the effect was reversible after DIM removal. These observations support our findings that DIM directly inhibited topoisomerase activity. Topoisomerases

have long been recognized as important enzymes in DNA replication to relieve DNA supercoiling caused by the moving replication fork. Consequently, the inhibition of topoisomerases will lead to the blockade of DNA synthesis (Berger et al., 1996; Champoux, 2001; Cortes et al., 2003; Topcu, 2001; Wang, 2002).

DIM is less active towards human topo II β than topo II α . It is known that human topo II α and β are encoded by different genes with 68% homology at amino acid level. Although they share ATP-dependent strand passage activity, topo II β relaxes DNA in a more processive manner (Austin and Marsh, 1998). Previous experiments have showed that the two enzyme isoforms have different sensitivities to topoisomerase-targeting drugs. For merbarone, a catalytic topo II inhibitor, topo II β is eight to ten times less sensitive than α (Austin and Marsh, 1998; Fortune and Osheroff, 1998). The inhibitory effect of DIM against topo II α is important, given crucial role of this enzyme in mitotic chromosome segregation (Berger et al., 1996; Chang et al., 2003; Osheroff, 1986; Osheroff et al., 1983). Between the two isoforms of vertebrate topo II, topo II α is more widely studied and thought to be more essential for mitotic chromosome separation due to its peak expression in mitosis and its association with chromosomes from metaphase to telophase. Our results clearly showed that DIM strongly inhibited topo II α . Not only was mitosis severely retarded by DIM, but also the abnormal chromosome morphology was seen after DIM treatment. These observations, together with the strong inhibitory effect of DIM on DNA synthesis, provide evidence that DIM functions as topoisomerase inhibitor *in vivo*.

We propose that DIM inhibits human topo II α by targeting the step of ATP hydrolysis (Berger et al., 1996; Osheroff, 1986; Osheroff et al., 1983). Recently, a protein clamp model has been illustrated for eukaryotic topo II, in which a homodimeric enzyme acts as an ATP-modulated protein clamp to hold the DNA substrate. ATP binding closes the clamp, and ATP hydrolysis reopens the clamp to release the DNA. Antitumor drugs such as bisdioxopiperazines inhibit topo II by inhibiting ATP hydrolysis thus

trapping the enzyme in the form of a closed protein clamp (Berger et al., 1996; Osheroff, 1986; Roca et al., 1994). We performed topo II α -mediated ATPase assay using thin layer chromatography and found that DIM concentration-dependently inhibited topo II α -mediated ATP hydrolysis and the inhibition was more complete when lower amount of enzyme was present in the reaction mixture. This observation also helps us to explain why DIM 50 μ M could completely inhibit topo II α activity in the supercoiled DNA relaxation assay, where only one unit of topo II α was used.

Our observation that topo II α is a target of DIM action is consistent with available information on the distribution of the compound in cultured cells. In a previous study to determine the subcellular distribution of DIM, we found that DIM was very rapidly taken into the cultured cells and was highly concentrated in the nuclear fraction as well as the lipid membrane fraction of the cells (unpublished data). These observations suggested that DIM could reach its target—nuclear topoisomerases.

It is been known that rapidly proliferating and transformed cells contain higher levels of topoisomerases, which makes them more sensitive to topoisomerase inhibition (Bronstein et al., 1996; Lynch et al., 1997; Nakopoulou et al., 2001; van der Zee et al., 1994). Two classes of topoisomerase inhibitors have been characterized—topoisomerase poisons, which stabilize DNA cleavage complex and induce DNA damage, and the catalytic inhibitors, which include structurally diverse compounds interfering with different stages of the catalytic cycle, but do not induce DNA cleavage complex formation (Larsen et al., 2003). We provide both *in vitro* and cell culture evidence to classify DIM as a catalytic inhibitor. Catalytic topoisomerase inhibitors are now being clinically used as antineoplastic agents (aclarbicin and MST-16), cardioprotectors (ICRF-187), or modulators in order to increase the efficacy of other agents (suramin and novobiocin) (Larsen et al., 2003). Increasing evidence suggests that topoisomerase inhibition can regulate gene promoter activity by altering local DNA topology (Collins et al., 2001; Narayana et al., 1998). As revealed by the studies of topoisomerase II inhibitor

etoposide and salvicine, topoisomerase II inhibition may be able to regulate the expression of genes involved in tumor migration, invasion and metastasis (Chang et al., 2005; Lang et al., 2005; Larsen et al., 2003; Mashimo et al., 2000). In our preliminary study, DIM inhibited human primary endothelial cell migration in culture and decreased blood vessel formation in xenograft solid human breast tumors (Chang et al., 2005). Although the mechanisms of this inhibition are under further investigation, it is possible that inhibition of DNA topoisomerase changes the expression of genes involved in tumor metastasis.

In conclusion, the results of our study indicate that DIM is a catalytic topo II α inhibitor that exerts cytostatic effects on hepatoma cells and interferes with several phases of the cell cycle. Our study identified a further important mode of action for this intriguing dietary component that might be exploited for the therapeutic development.

ACKNOWLEDGMENTS

We express our appreciation to members of both the Bjeldanes and Firestone laboratories for their helpful comments throughout the duration of this work. We are also thankful to Hector Nolla for his assistance in flow cytometry assay and Steven Ruzin and Denise Schichnes for their help in fluorescence imaging.

REFERENCE

- Austin CA and Marsh KL (1998) Eukaryotic DNA topoisomerase II beta. *Bioessays* **20**:215-226.
- Berger JM, Gamblin SJ, Harrison SC and Wang JC (1996) Structure and mechanism of DNA topoisomerase II. *Nature* **379**:225-232.
- Bronstein IB, Vorobyev S, Timofeev A, Jolles CJ, Alder SL and Holden JA (1996) Elevations of DNA topoisomerase I catalytic activity and immunoprotein in human malignancies. *Oncol Res* **8**:17-25.
- Champoux JJ (2001) DNA topoisomerases: structure, function, and mechanism. *Annu Rev Biochem* **70**:369-413.
- Chang CJ, Goulding S, Earnshaw WC and Carmena M (2003) RNAi analysis reveals an unexpected role for topoisomerase II in chromosome arm congression to a metaphase plate. *J Cell Sci* **116**:4715-4726.
- Chang X, Tou JC, Hong C, Kim HA, Riby JE, Firestone GL and Bjeldanes LF (2005) 3,3'-Diindolylmethane inhibits angiogenesis and the growth of transplantable human breast carcinoma in athymic mice. *Carcinogenesis* **26**:771-778.
- Chen I, McDougal A, Wang F and Safe S (1998) Aryl hydrocarbon receptor-mediated antiestrogenic and antitumorigenic activity of diindolylmethane. *Carcinogenesis* **19**:1631-1639.
- Chen I, Safe S and Bjeldanes L (1996) Indole-3-carbinol and diindolylmethane as aryl hydrocarbon (Ah) receptor agonists and antagonists in T47D human breast cancer cells. *Biochem Pharmacol* **51**:1069-1076.
- Clarke DJ, Johnson RT and Downes CS (1993) Topoisomerase II inhibition prevents anaphase chromatid segregation in mammalian cells independently of the generation of DNA strand breaks. *J Cell Sci* **105 (Pt 2)**:563-569.
- Collins I, Weber A and Levens D (2001) Transcriptional consequences of topoisomerase inhibition. *Mol Cell Biol* **21**:8437-8451.
- Cortes F, Pastor N, Mateos S and Dominguez I (2003) Roles of DNA topoisomerases in chromosome segregation and mitosis. *Mutat Res* **543**:59-66.
- Dashwood RH, Fong AT, Arbogast DN, Bjeldanes LF, Hendricks JD and Bailey GS (1994) Anticarcinogenic activity of indole-3-carbinol acid products: ultrasensitive bioassay by trout embryo microinjection. *Cancer Res* **54**:3617-3619.
- De Kruif CA, Marsman JW, Venekamp JC, Falke HE, Noordhoek J, Blaauboer BJ and Wortelboer HM (1991) Structure elucidation of acid reaction products of indole-3-carbinol: detection in vivo and enzyme induction in vitro. *Chem Biol Interact* **80**:303-315.
- Denny WA and Baguley BC (2003) Dual topoisomerase I/II inhibitors in cancer therapy. *Curr Top Med Chem* **3**:339-353.

Firestone GL and Bjeldanes LF (2003) Indole-3-carbinol and 3,3'-diindolylmethane antiproliferative signaling pathways control cell-cycle gene transcription in human breast cancer cells by regulating promoter-Sp1 transcription factor interactions. *J Nutr* **133**:2448S-2455S.

Fortune JM and Osheroff N (1998) Merbarone inhibits the catalytic activity of human topoisomerase II α by blocking DNA cleavage. *J Biol Chem* **273**:17643-17650.

Gross-Steinmeyer K, Stapleton PL, Liu F, Tracy JH, Bammler TK, Quigley SD, Farin FM, Buhler DR, Safe SH, Strom SC and Eaton DL (2004) Phytochemical-induced changes in gene expression of carcinogen-metabolizing enzymes in cultured human primary hepatocytes. *Xenobiotica* **34**:619-632.

He YH, Smale MH and Schut HA (1997) Chemopreventive properties of indole-3-carbinol (I3C): inhibition of DNA adduct formation of the dietary carcinogen, 2-amino-1-methyl-6-phenylimidazo [4,5-b]pyridine (PhIP), in female F344 rats. *J Cell Biochem Suppl* **27**:42-51.

Lake BG, Tredger JM, Renwick AB, Barton PT and Price RJ (1998) 3,3'-Diindolylmethane induces CYP1A2 in cultured precision-cut human liver slices. *Xenobiotica* **28**:803-811.

Lang JY, Chen H, Zhou J, Zhang YX, Zhang XW, Li MH, Lin LP, Zhang JS, Waalkes MP and Ding J (2005) Antimetastatic effect of salvicine on human breast cancer MDA-MB-435 orthotopic xenograft is closely related to Rho-dependent pathway. *Clin Cancer Res* **11**:3455-3464.

Larsen AK, Escargueil AE and Skladanowski A (2003) Catalytic topoisomerase II inhibitors in cancer therapy. *Pharmacol Ther* **99**:167-181.

Leibelt DA, Hedstrom OR, Fischer KA, Pereira CB and Williams DE (2003) Evaluation of chronic dietary exposure to indole-3-carbinol and absorption-enhanced 3,3'-diindolylmethane in sprague-dawley rats. *Toxicol Sci* **74**:10-21.

Lynch BJ, Guinee DG, Jr. and Holden JA (1997) Human DNA topoisomerase II- α : a new marker of cell proliferation in invasive breast cancer. *Hum Pathol* **28**:1180-1188.

Mashimo T, Bandyopadhyay S, Goodarzi G, Watabe M, Pai SK, Gross SC and Watabe K (2000) Activation of the tumor metastasis suppressor gene, KAI1, by etoposide is mediated by p53 and c-Jun genes. *Biochem Biophys Res Commun* **274**:370-376.

Nakopoulou L, Zervas A, Lazaris AC, Constantinides C, Stravodimos C, Davaris P and Dimopoulos C (2001) Predictive value of topoisomerase II α immunostaining in urothelial bladder carcinoma. *J Clin Pathol* **54**:309-313.

Narayana A, Khodarev N, Walter S and Vaughan AT (1998) Synchronous block in DNA synthesis initiation with change in chromatin topology mediated by VP16. *DNA Cell Biol* **17**:613-619.

Oganesian A, Hendricks JD and Williams DE (1997) Long term dietary indole-3-carbinol inhibits diethylnitrosamine-initiated hepatocarcinogenesis in the infant mouse model. *Cancer Lett* **118**:87-94.

Osheroff N (1986) Eukaryotic topoisomerase II. Characterization of enzyme turnover. *J Biol Chem* **261**:9944-9950.

Osheroff N, Shelton ER and Brutlag DL (1983) DNA topoisomerase II from *Drosophila melanogaster*. Relaxation of supercoiled DNA. *J Biol Chem* **258**:9536-9543.

Pommier Y, Pourquier P, Fan Y and Strumberg D (1998) Mechanism of action of eukaryotic DNA topoisomerase I and drugs targeted to the enzyme. *Biochim Biophys Acta* **1400**:83-105.

Renwick AB, Mistry H, Barton PT, Mallet F, Price RJ, Beamand JA and Lake BG (1999) Effect of some indole derivatives on xenobiotic metabolism and xenobiotic-induced toxicity in cultured rat liver slices. *Food Chem Toxicol* **37**:609-618.

Roca J, Ishida R, Berger JM, Andoh T and Wang JC (1994) Antitumor bisdioxopiperazines inhibit yeast DNA topoisomerase II by trapping the enzyme in the form of a closed protein clamp. *Proc Natl Acad Sci U S A* **91**:1781-1785.

Sanderson JT, Slobbe L, Lansbergen GW, Safe S and van den Berg M (2001) 2,3,7,8-Tetrachlorodibenzo-p-dioxin and diindolylmethanes differentially induce cytochrome P450 1A1, 1B1, and 19 in H295R human adrenocortical carcinoma cells. *Toxicol Sci* **61**:40-48.

Sorensen BS, Sinding J, Andersen AH, Alsner J, Jensen PB and Westergaard O (1992) Mode of action of topoisomerase II-targeting agents at a specific DNA sequence. Uncoupling the DNA binding, cleavage and religation events. *J Mol Biol* **228**:778-786.

Staub RE, Feng C, Onisko B, Bailey GS, Firestone GL and Bjeldanes LF (2002) Fate of indole-3-carbinol in cultured human breast tumor cells. *Chem Res Toxicol* **15**:101-109.

Takahashi N, Dashwood RH, Bjeldanes LF, Williams DE and Bailey GS (1995) Mechanisms of indole-3-carbinol (I3C) anticarcinogenesis: inhibition of aflatoxin B1-DNA adduction and mutagenesis by I3C acid condensation products. *Food Chem Toxicol* **33**:851-857.

Topcu Z (2001) DNA topoisomerases as targets for anticancer drugs. *J Clin Pharm Ther* **26**:405-416.

van der Zee AG, de Jong S, Keith WN, Hollema H, Boonstra H and de Vries EG (1994) Quantitative and qualitative aspects of topoisomerase I and II alpha and beta in untreated and platinum/cyclophosphamide treated malignant ovarian tumors. *Cancer Res* **54**:749-755.

Wang JC (2002) Cellular roles of DNA topoisomerases: a molecular perspective. *Nat Rev Mol Cell Biol* **3**:430-440.

FOOTNOTES

This research was supported by the Department of Defense, Army Breast Cancer Research Program Grant DAMD17-96-1-6149 and by grants CA69056 and CA102360 from the National Institutes of Health.

LEGENDS FOR FIGURES

Figure 1. DIM inhibited HepG2 cell proliferation. (A) DIM concentration-dependently inhibited the growth of HepG2 cells as measured by cell number counting every 24 hours for up to 72 hours. Reported values were mean \pm S.D. from one experiment with 3 replicates. The results are representative of two duplicate runs. (B) Confocal microscopy of the morphological changes in HepG2 nuclei after 24 hours of 75 μ M DIM treatment. The slides were prepared as described in “Materials and methods”.

Figure 2. DIM interacted with DNA *in vitro*. (A) DIM fluoresced concentration-dependently when excited at 280 nm. From 1-6: DIM 50 μ M, 30 μ M, 10 μ M, 5 μ M, 1 μ M, 0 μ M. (B) Salmon sperm DNA concentration-dependently quenched DIM fluorescence at 370 nm. DIM concentration was 30 μ M. 1-8: 0-14 μ g DNA at 2 μ g intervals. (C) DIM was a weak DNA intercalator compared with m-AMSA as determined by ethidium bromide displacement assay. The asterisks indicate significant difference versus vehicle control DMSO (* p < 0.05).

Figure 3. Effects of DIM on human topo I, II α and II β activities. (A) DIM partially inhibited topo I-mediated supercoiled pBR322 DNA relaxation. (B) DIM concentration-dependently inhibited topo II α -mediated supercoiled pRYG DNA relaxation. (C) DIM concentration-dependently inhibited topo II α -mediated KDNA decatenation. (D) DIM did not inhibit topo II β -mediated KDNA relaxation until DIM concentration reached 75 μ M. All experiments were carried out according to Topogen Inc. kit instructions. Reactions contained 1 U of enzyme, 0.2 μ g of DNA substrate, and different concentrations of drugs dissolved in DMSO (1% final concentration v/v). Different topological forms exhibited different mobility as indicated in the figure. SC: supercoiled; RX: relaxed; cat.: catenated; decat.:

decatenated.

Figure 4. DIM inhibited synchronized HepG2 cell cycle progression. HepG2 cells were synchronized at G1-S boundary by double thymidine block as described in “Materials and methods”. Two hours after release from G1-S block, HepG2 cells were treated with either DMSO (0.1%) or different concentrations of DIM. The samples were collected for flow cytometry DNA content analysis at 0 hour, 5 hours, 9 hours and 12 hours after the release. The position of 2N and 4N DNA are indicated.

Figure 5. DIM inhibited DNA synthesis in HepG2 cells. DIM inhibited DNA synthesis within 1 hour of treatment and the effects were reversible after the removal of DIM. HepG2 cells were treated with DMSO (0.1%) or different concentrations of DIM. ^3H -dT incorporation was measured within the first hour of treatment. To examine whether the DNA synthesis inhibition was reversible, after 1 hour of DIM exposure, cells were washed with PBS and re-incubated in DIM-free fresh medium. ^3H -dT incorporation was measured again during the first hour or the fourth hour of recovery. Asterisks indicate a significant decrease versus vehicle control DMSO ($*p < 0.05$). \dagger indicates a significant increase versus no DIM removal ($\dagger p < 0.05$). \ddagger indicates a significant increase versus 1 hour after DIM removal ($\ddagger p < 0.05$).

Figure 6. DIM blocked mitosis in HepG2 cells. HepG2 cells were synchronized in prometaphase by 24-hour treatment with 40 ng/ml nocodazole. Immediately after release, cells were seeded onto poly-L-lysine-coated slides and treated with either 0.1% DMSO, DIM 30 μM , DIM 50 μM or aclarubicin 10 μM . After 4 hours, the cells were fixed and stained with 2 $\mu\text{g/ml}$ of DAPI. For each example, the percentage of the remaining mitotic cells was counted under fluorescent microscope. The percentage of

mitotic cells at the time of release was set as 100%. Reported values were mean \pm S.D. from the results of counting at least 400 cells. The asterisks indicate significant difference versus DMSO-treated cells ($*p < 0.05$).

Figure 7. DIM interfered with mitotic chromosome separation in HepG2 cells. (A-C) DIM blocked mitotic chromosome separation. The slides were prepared in the same way as in Figure 6. The digital images were obtained with Zeiss LSM510 Meta confocal microscope. A: DMSO; B: aclarubicin 10 μ M; C: DIM 50 μ M. Long arrows indicate cells still in mitosis; short arrows indicate irregular nuclei after DIM treatment. (D-G) DIM induced chromosomal bridges during anaphase chromosome separation. D: DMSO; E: aclarubicin 10 μ M; F and G: DIM 50 μ M.

Figure 8. DIM was not a topoisomerase poison. (A and B) DIM did not stabilize either topo I or topo II α -induced DNA cleavage complex *in vitro*. All experiments were carried out according to Topogen Inc. kit instructions. Reactions contained 10 U of topo I or II α , 0.2 μ g of plasmid DNA, and different concentrations of drugs dissolved in DMSO (1% final concentration v/v). Different topological forms exhibited different mobility as indicated in the figure. OC: open circular; SC: supercoiled; RX: relaxed; LI: linear. (C, D and E) DIM did not produce DNA breakage in HepG2 cells after 6 hours of treatment. HepG2 cells were treated with indicated concentrations of drugs for indicated times. Single and double-stranded DNA breaks were measured by single gel electrophoresis assay as described by Trevigen Inc. protocol.

Figure 9. DIM did not prevent etoposide-induced DNA cleavage complex formation. The experiment was carried out according to Topogen Inc. kit instructions. Different concentrations of DIM

and 100 μ M etoposide were coincubated with 10 U of topo II α , 0.2 μ g of supercoiled pRYG DNA for 30 min. Aclarubicin (acla) was used as positive control to prevent etoposide-induced DNA cleavage complex. Different topological forms exhibited different mobility as indicated in the figure. OC: open circular; SC: supercoiled; RX: relaxed; LI: linear.

Figure 10. DIM inhibited topo II α -mediated ATP hydrolysis. ATP hydrolysis was measured by thin layer chromatography as described in “Materials and methods”. The areas corresponding to the free radioactive inorganic phosphate were cut out and quantified by scintillation counting. Data are the mean \pm S.D. of triplicates for each concentration. The asterisks indicate significant difference versus vehicle control (* p < 0.05).

Figure 1

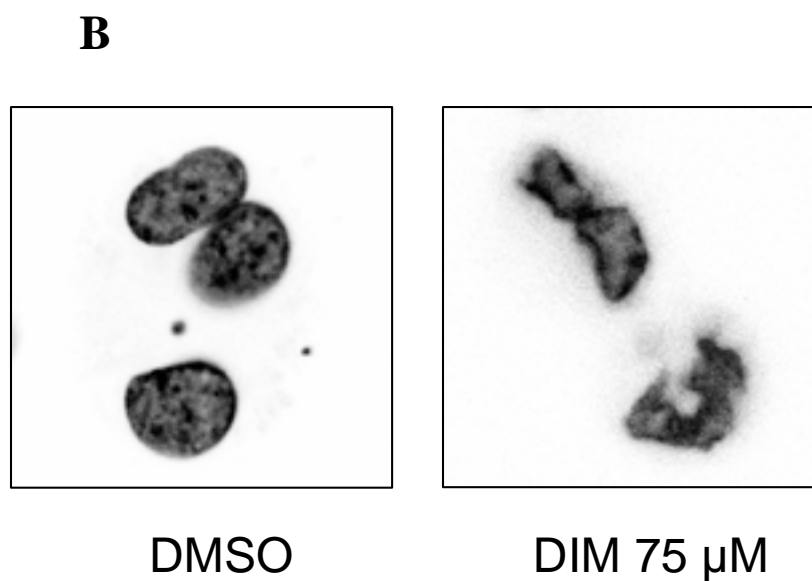
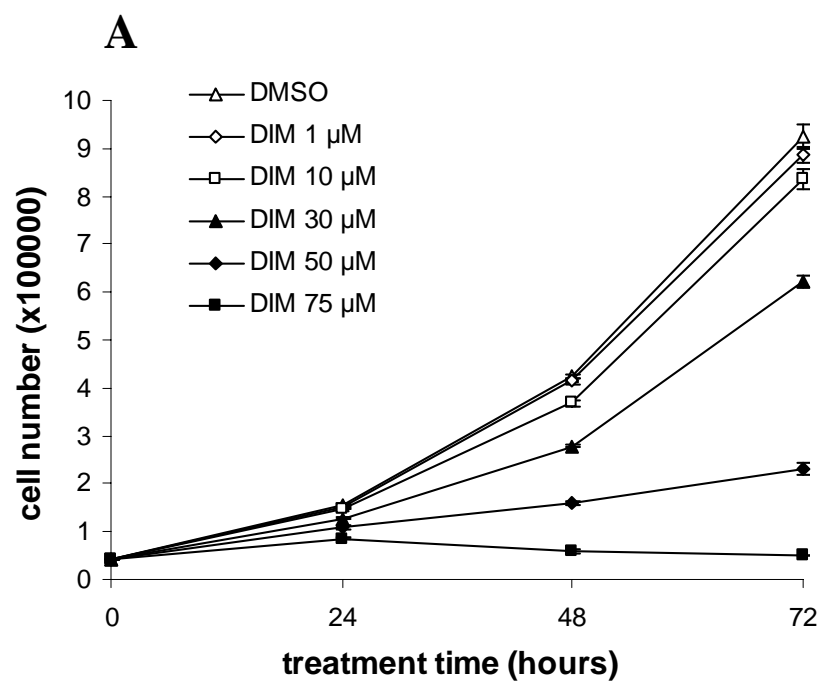


Figure 2

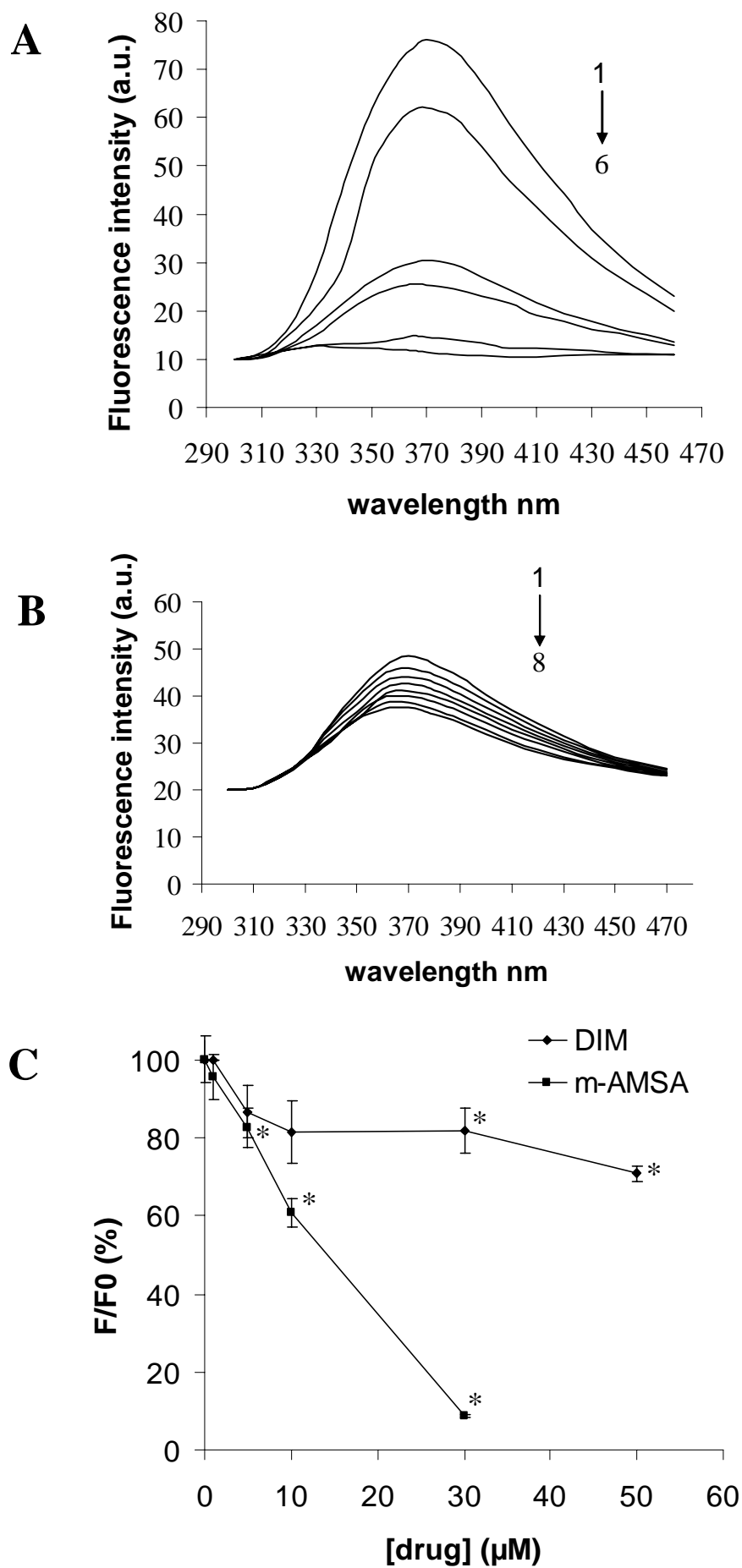


Figure 3

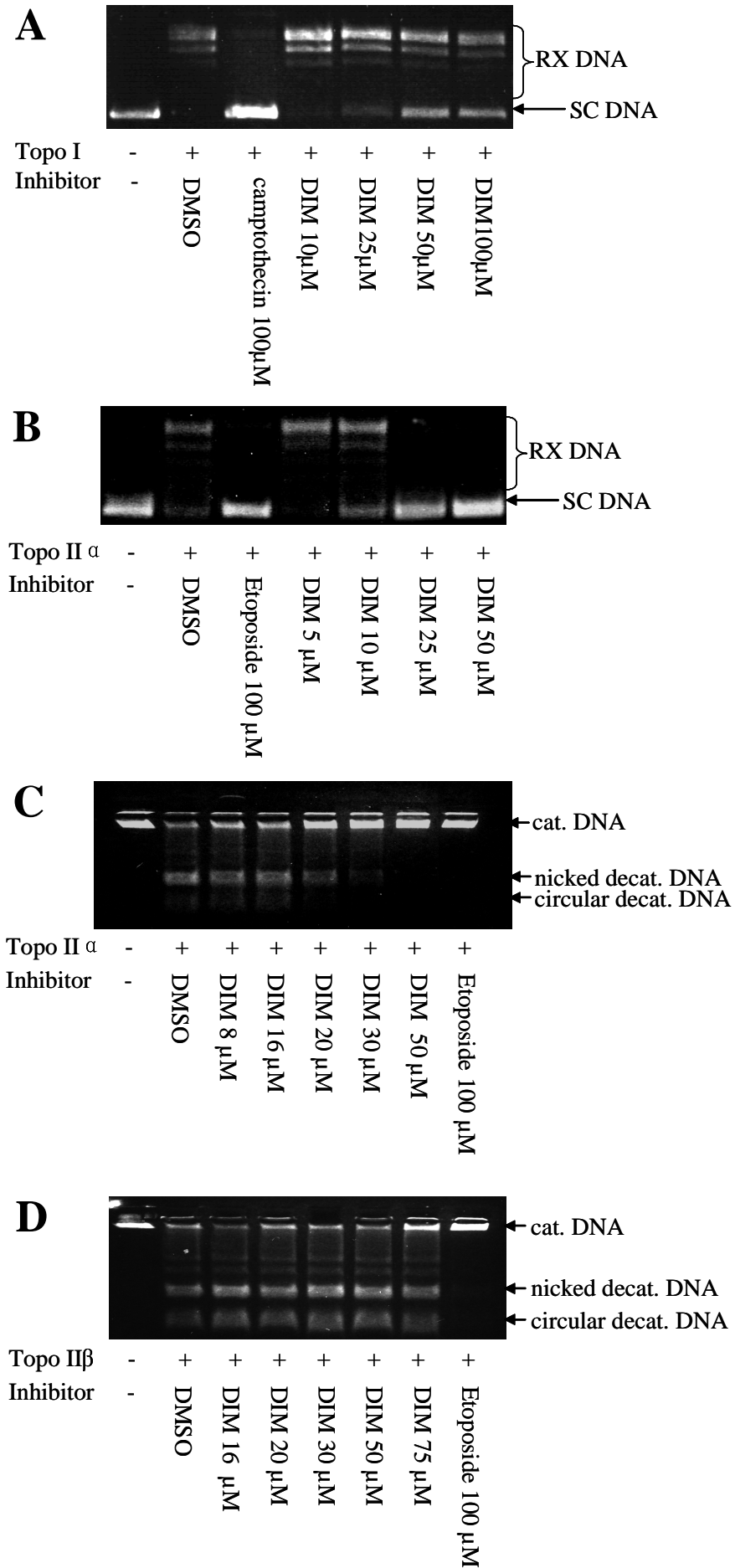


Figure 4

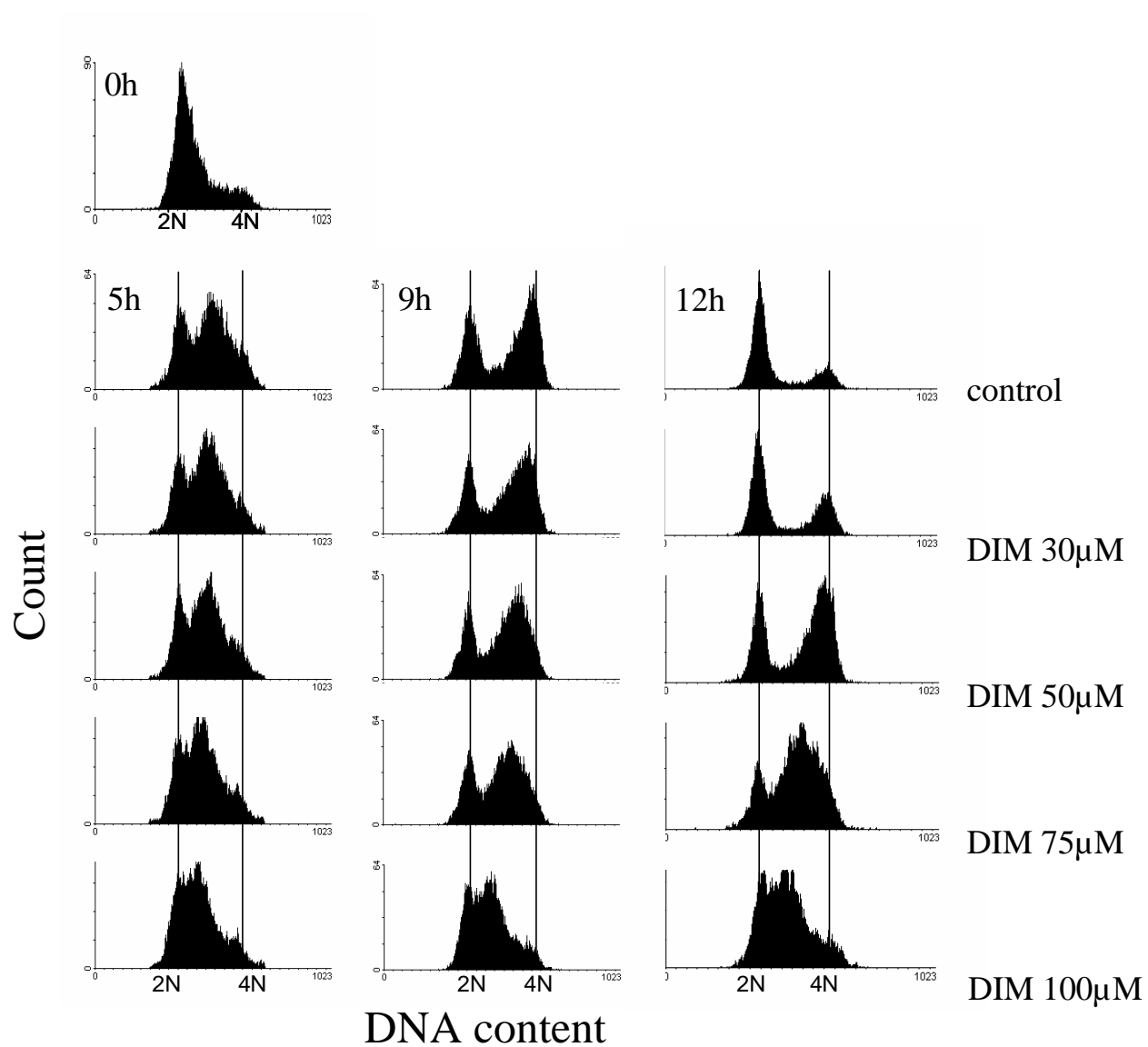


Figure 5

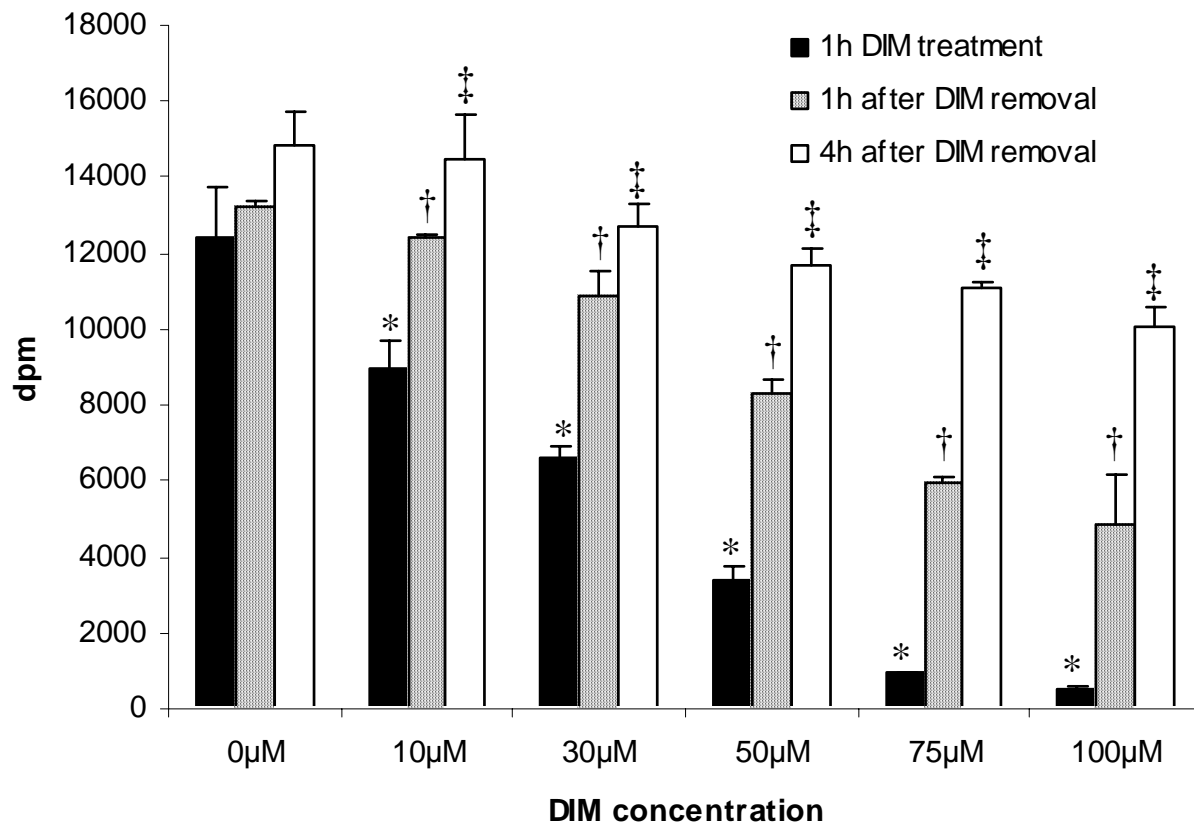


Figure 6

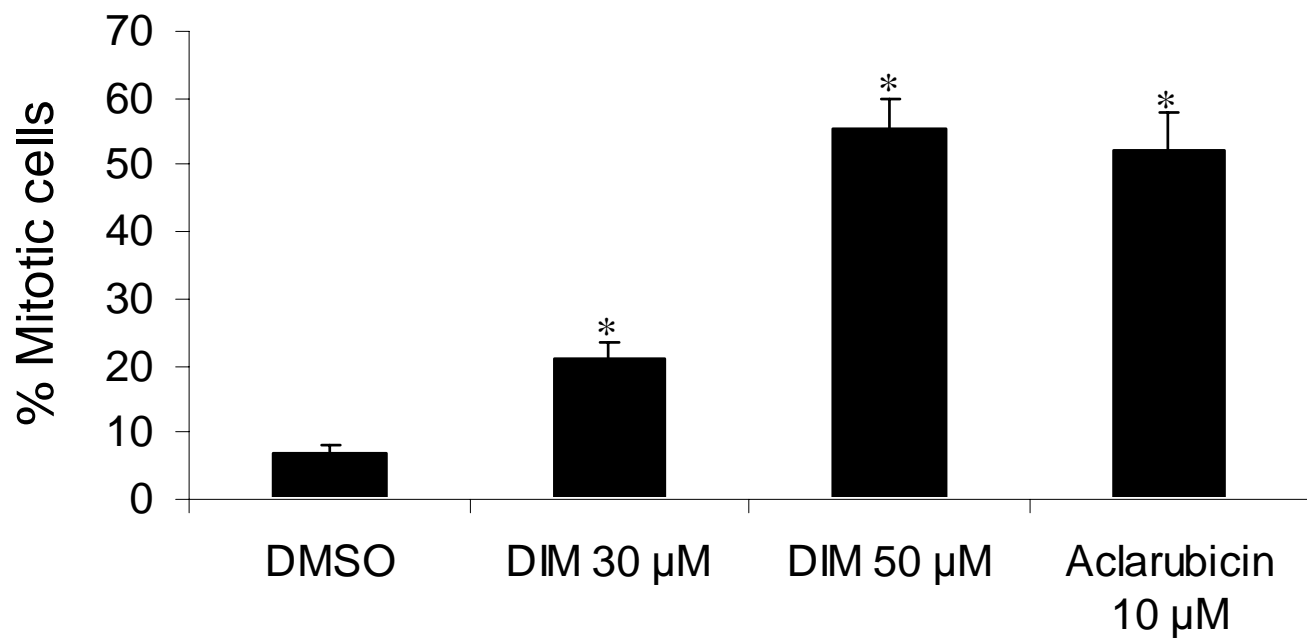


Figure 7

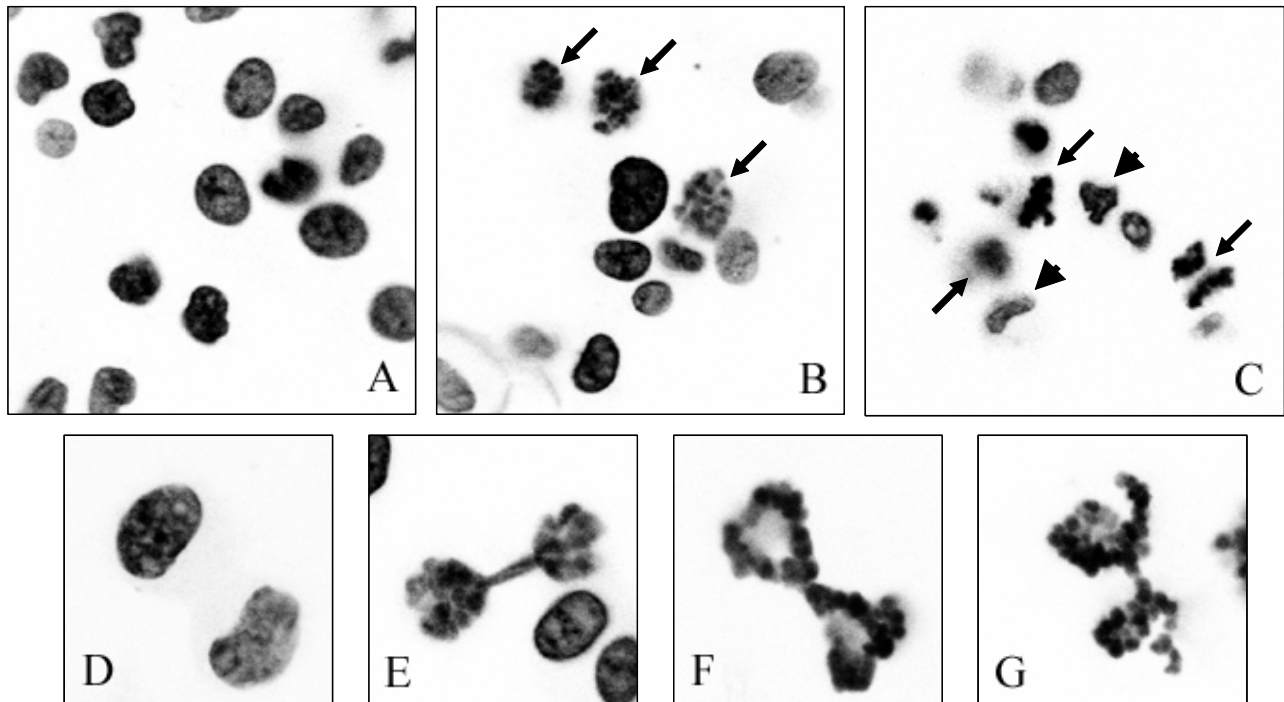


Figure 8

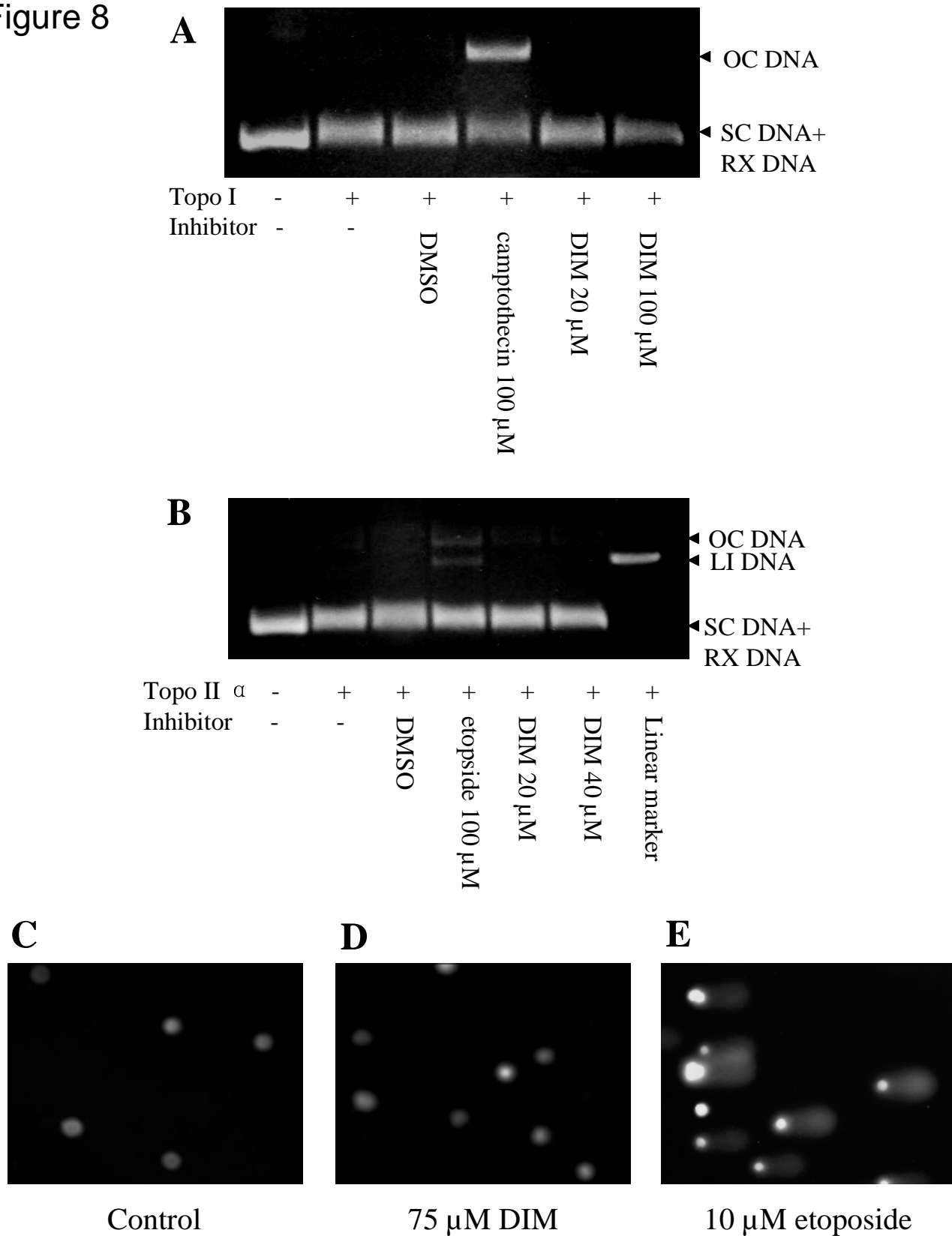


Figure 9

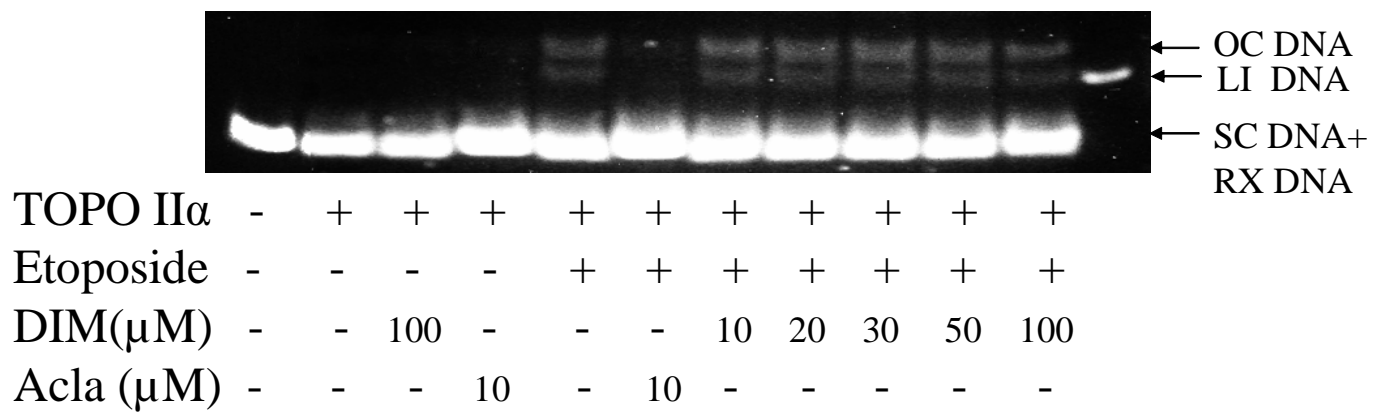


Figure 10

